JTTEE5 19:866–872
DOI: 10.1007/s11666-010-9488-x
1059-9630/$19.00 © ASM International

Peer Reviewed

Characterization of Thermal Spray Coatings for Cylinder Running Surfaces of Diesel Engines

Mareike Hahn and Alfons Fischer

(Submitted July 9, 2009; in revised form August 24, 2009)

Future demands of diesel engines are about low-friction and wear-resistant materials in order to increase the efficiency and achieve environmentally sound solutions. Thus, thermally sprayed Fe-base coatings are investigated for application as cylinder running surfaces in cast aluminum crankcases. They should allow the desired combination of structural, productional, and topographical properties required in Diesel engines. To understand the influence of the characteristic microstructures on the integrity of the composites the coatings have to be examined in laboratory tests in terms of different loading situations. Cavitation tests were carried out where the tribological stability of these coatings and their ability to resist high-frequency cyclic impact stresses are revealed. Composite samples (base material and coating) were investigated in terms of crack initiation in a scanning electron microscope with an in situ 3-point-bending test. The endurance under cyclic mechanical stresses was tested with a 4-point-bending stress controlled test.

Keywords coating characteristics, Fe-base coatings, thermal spray

1. Introduction

Versatile thermal spray processes and material combinations have been applied in automotive engineering. Wear protection as well as reducing friction are of major concern and led to the development of powder and wire consumables adapted to the specific features of the different spraying processes for manufacturing and repair (Ref 1). The structure and, therefore, the properties of metal sprayed coatings are governed by the thermal and kinetic energy introduced. Particle velocities might vary from 150 m/s for Twin Wire Arc Spraying (TWAS), 450 m/s for Plasma Transferred Wire Arc (PTWA) up to 750 m/s for High Velocity Oxygen Fuel (HVOF). Mean particle temperatures are about 2000 °C for TWAS and PTWA but kept in the vicinity of the material melting point within HVOF spraying. This leads to differing characteristic features (particles size, pore and oxide fraction and size, lamella or splat thickness) within such coatings (Ref 2-4). Coating characteristics depend on bonding between the splats and the substrate as well as between the individual splats whereas voids and splat grain boundaries play a significant role in fatigue behavior of these coatings (Ref 5).

Mareike Hahn and **Alfons Fischer**, University of Duisburg-Essen, Institute of Product Engineering, Materials Science and Engineering, Lotharstr. 1, 47057 Duisburg, Germany. Contact e-mails: mareike.hahn@uni-due.de and alfons.fischer@uni-due.de.

Hitherto low alloyed carbon steels with 0.9 wt.% carbon have been successfully used for cylinder coatings. Many wear-resistant coatings make use of hard phases which are either introduced by alloying (e.g., C and B for carbides and borides) or by the atmosphere during spraying (e.g., O for oxides). A prototype Fe-base alloy with chromium and boron was developed as a filler wire feedstock by Durum Verschleißschutz GmbH which due to the rapid cooling within the spraying processes should solidify into a nanocrystalline (nc) or even amorphous matrix. Nanocrystalline metals possess some appealing mechanical properties such as high strength and beneficial tribologic properties and are for this reason considered for future application in diesel engines.

Boundary lubrication is assumed in the cylinder-ring interface at the reversal points of the piston, the top and bottom dead center. There the lubricant film breaks down due to the low sliding velocity. Within a cylinder bore the coatings undergo high-temperature corrosion above the top dead center (TDC), impact and sliding wear at TDC and the bottom dead center (BDC) as well as reciprocating sliding wear within the stroke. Motor tests as well as reciprocating sliding wear tests are currently carried out. First results on the microstructural alterations in FeC coated cylinders in different contact zones after motor tests are published in Hahn et al. (Ref 6, 7). Mechanically and chemically caused changes are investigated by means of transmission electron microscopy (TEM) and energy filtered TEM (EFTEM).

Apart from tribological stresses the increasing ignition pressures of modern motor concepts bring about mechanical fatigue within the upper and lower regions of a cylinder, while knocking will lead to additional oscillatory impacts. Thus, such coatings have to be examined at these loading situations in laboratory before motor tests.

From other wear-resistant materials it is known that crack initiation is accelerated and early unstable crack growth is likely. Fatigue mechanisms in coatings result in cohesive (crack initiation and growth which leads to spalling) and adhesive failure (delamination of large fractions of the coating from the substrate) (Ref 8). Vertical cracks might propagate into the substrate material and provoke collateral damages by fracture or leakage. Coating defects and residual stresses contribute to reduce bond strength and, therefore, are responsible for failure during operation (Ref 9).

Cavitation does not occur in engine operation but knock conditions and impact of piston rings cause high-impact stresses that can be simulated by cavitation tests. The test results should reveal the tribological stability of these coatings and their ability to resist high-frequency cyclic impact stresses. Crack initiation and propagation are observed in a scanning electron microscope during an in situ 3-point-bending test. Fatigue tests were carried out as 4-point-bending cyclic tests whereas the flexural stiffness refers to the mechanical properties of these layered composites. Surface fatigue during cavitation as well as crack initiation and propagation are investigated and brought into relation to the relevant microstructure.

2. Materials and Experimental Methods

2.1 Materials

Different coating materials are thermally sprayed onto the bore of a 84 mm diameter Al-alloy pressure casted cylinder (AlMgSi EN AW-6060) by means of the above-mentioned thermal spray processes. Coating materials are a commercial steel wire with 0.8 wt.% C and a prototype Fe-base alloy with Cr, C, and B (FeCr19C0.1B1.6) provided as a filler wire. TWAS samples for this investigation were sprayed by Daimler, Research and Development, Ulm, the HVOF samples were provided by GTV, Luckenbach, and the PTWA samples by IOT, RWTH Aachen. Spraying parameters for the prototype feedstock have to be investigated. Parameters for PTWA spraying of conventional steel compared to the prototype feedstock are published by Bobzin et al. (Ref 2).

Before spraying surfaces have to be activated. This is done by either high-pressure water jet blasting or a mechanical roughening process (mrp). The water is accelerated toward the substrate's surface with high-kinetic energy that partially removes the surface and leaves a finely structured topography, characterized by the required undercuts. The second activating process is a newly developed fine milling process with a polycrystalline diamond cutting tool that creates a so called ''dovetail''-like profile. This special profile secures a strong adhesion between coating and aluminum substrate (Ref 10).

The surface topography was manufactured by honing, whereas the honing procedure was optimized for the prototype coating by Gehring GmbH, Ostfildern. The coating thickness was thereby machined to an average of 150 ± 20 μm.

The splats in the layered texture of the sprayed coatings consist of several smaller grains. Additional phases exist either by alloying (hard phases like borides) or due to the spraying process (oxide particles), while the latter must not be detrimental for some desired properties. Depending on the spray process and parameters, the splat particle size as well as the underlying grain size can vary over about an order of magnitude (Fig. 1).

For the TWAS sprayed FeC coatings the splats consist of microcrystalline ferrite with fine-lamellar cementite (Fig. 1a). Because of the high solidification rate this microstructure can be attributed to be troostite. Oxide phases are FeO (wuestite) grains or precipitates. The matrix of HVOF FeC coatings consists of microcrystalline (μc) ferrite or wuestite; nc precipitates are calculated from diffraction patterns as either wuestite or ferrite (Fig. 1b). Near eutectic FeCrCB alloys tend to solidify either

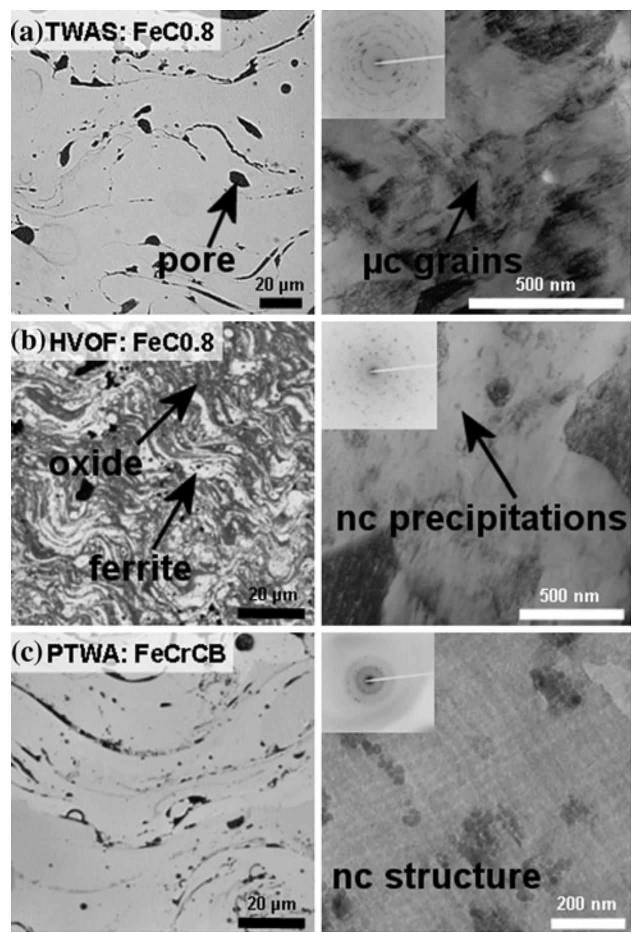

Fig. 1 Microstructures of the different thermally sprayed coatings: (a) TWAS FeC0.8 coating with coarse splats consisting of a μc α-Fe matrix with fine-lamellar Fe3C and nc precipitations of FeO, (b) HVOF FeC0.8 coating with fine splats consisting of a μc α-Fe or FeO matrix and accordingly nc precipitations of α-Fe or FeO, (c) The PTWA FeCr19C0.1B1.6 coating has a predominantly amorphous or nc matrix and some μc oxides

amorphous or nc under a high solidification rate. After solidification, the crystallization is hindered because of either the lack of nucleation sites or the very slow growth rate of crystals (Ref 11). Thus, the PTWA FeCrCB coating shows a mixture of an amorphous and nc matrix with borides of the composition $M_{23}B_6$ (M = Fe, Cr) (Fig. 1c). The further analysis of the precise composition of these phases is subject to current investigations.

2.2 Cavitation Tests

The cavitation test rig is based on a 20 kHz generator (KLN Typ 512/1206, KLN Ultraschall AG, Heppenheim, Germany). Concave specimens of 20 by 20 mm^2 are cut from the coated cylinders and corresponding convex sonotrode tips were manufactured from a solution annealed austenitic high nitrogen steel X13CrMnMoN18-14-3 (1.4452). Specimens and sonotrode tips are adjusted at least 15 mm below the liquid's surface (distilled water at 20 °C) at a distance of 0.5 mm by means of a precision altimeter (Digimatic Height Gage 570, Mitutoyo, Japan). Temperature is controlled by a cryostat (RM6, Lauda, Germany). Before and after each test the specimens are ultrasonically cleaned in acetone and blow-dried afterward. Finally the weight is measured by means of a precision scale (AC211S, Sartorius, Göttingen, Germany) with a resolution of 10^{-5} g. The mean cumulative weight loss of three runs of similar specimens is then plotted versus the testing time. The cavitated surfaces are examined by scanning electron microscopy.

2.3 In Situ Bending Tests

The in situ bending apparatus performs a 3-point-bending test whereas specimens can be investigated in top- or sideview. In topview assembly bending causes tension stresses in the coating. In sideview assembly substrate and coating are under tensile load. Specimens are cut lengthwise from the coated cylinder with a size of 40 by 4.55 by 3 mm. For sideview investigations the specimens are grinded and polished. All specimens are ultrasonically cleaned in acetone before investigation.

2.4 Fatigue Tests

Fatigue tests are carried out by using a servo hydraulic testing machine (S56, Schenk, Germany). Curved specimens are cut from the coated cylinders. The specimen size is defined as a quarter segment of a 30 mm height ring with a width of approx. 6 mm. For the tests the stress ratio is $R = 0.1$ with a nominal stress at the specimen center of $\sigma_{max} = 45$ MPa. The critical mean strain was first evaluated by implementing a cyclic incremental step test. Strains are measured using strain gauges applied onto the honed coating surface. At test start the applied load is slowly increased to the nominal load to avoid overloading and premature destruction of the samples. Test runs are then continued until 3×10^6 cycles.

3. Results

3.1 Cavitation Tests

Figure 2 shows the cumulative weight loss over testing time. The weight loss for the FeC coatings show a nearly identical gradient until 20 min testing time, then the HVOF FeC coating tends to a slightly lower weight loss. There is no incubation phase visible for all coating samples. The weight loss immediately starts with the beginning of the test. The PTWA FeCrCB coating shows the highest weight loss, which might be a first hint on the low ductility of this material. The SEM images of the worn surfaces show a distinct influence in cavitation erosion due to splat grain size. The HVOF coating benefits from its fine lamellar structure, accordingly the wear loss seems to take place more or less continuously on the entire surface. The coarser TWAS and PTWA coatings delaminate along the splat grain interfaces. On smoother surface areas local pitting is visible which is characteristic for cavitation of polished surfaces. The PTWA FeCrCB coating shows larger and rather deep craters which is not the case for the TWAS FeC coating.

Further details about the influence of the surface topography and motor oil as cavitation medium have been published previously (Ref 12).

3.2 In Situ Bend Tests

Figures 3 to 5 are showing how splat grain size and coating composition influence the crack propagation with increased load during 3-point-bending.

The coarse TWAS FeC coating exhibits mainly inter-splat cracks (Fig. 3). Especially oxide layers on splat surfaces, generated during spraying, promote cracking along the splat's interfaces. With increasing load cracks proceed along such interfaces until they extend into the substrate where local interfacial cracking occurs and finally the specimen is disrupted by crack propagation through the substrate.

Within HVOF FeC coatings one can observe a mixed inter- and trans-splat cracking. Vertical cracks could change direction to induce horizontal cracking when striking a splat boundary. From the topview image it can be assumed that microcracks are growing on another and therefore generate larger cracks (Fig. 4). Trans-splat cracking which normally leads to vertical cracks seems to derive from defects in the splats, namely oxides, whereas inter-splat cracking originates from the weak adhesion between the individual splats.

The PTWA FeCrCB coating exhibits mainly inter-splat cracks at low loads but with increasing load brittle microcracking leads to a mixed inter- and trans-splat cracking. The lower fracture toughness of the coating material gives rise to an abrupt and quick failure of the specimen at lower loads compared to TWAS and HVOF FeC coatings.

3.3 Fatigue Tests

Flexural stiffness values were calculated from the recorded data for both tension and compression sided bend

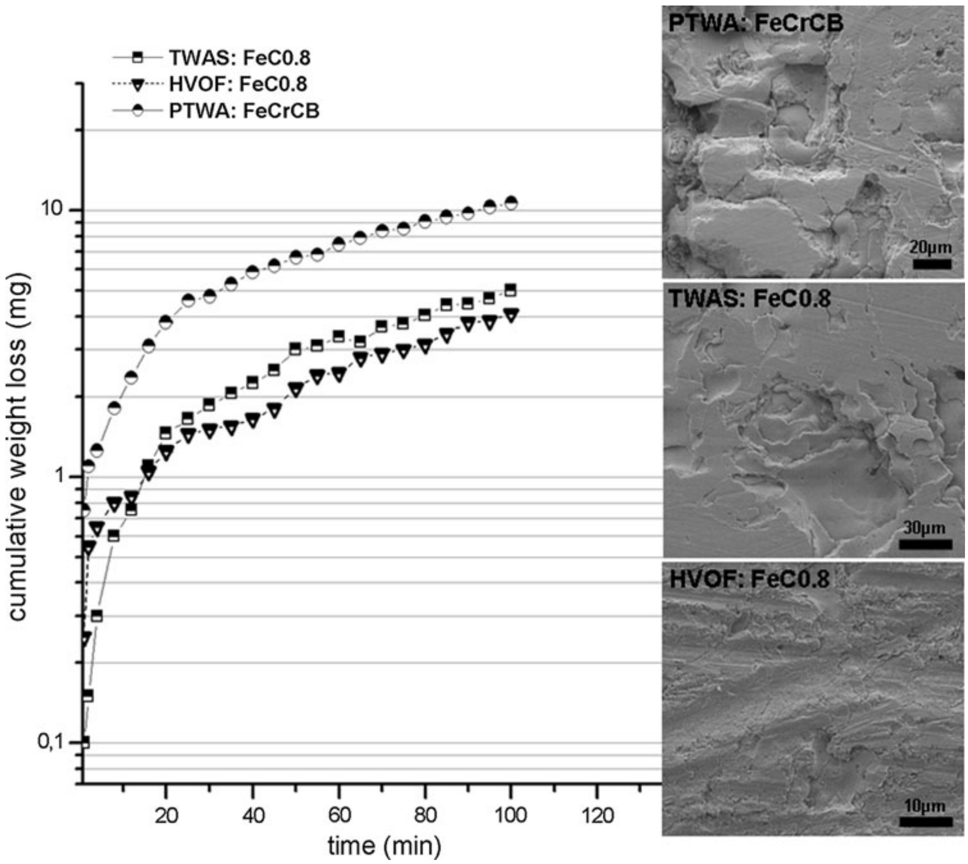

Fig. 2 Cumulative weight loss and wear appearances of the cavitated surfaces. The PTWA coating shows brittle cracking and localized craters. The TWAS coating delaminates along the splat boundaries. For the HVOF coating the wear loss appears continuously over the entire surface

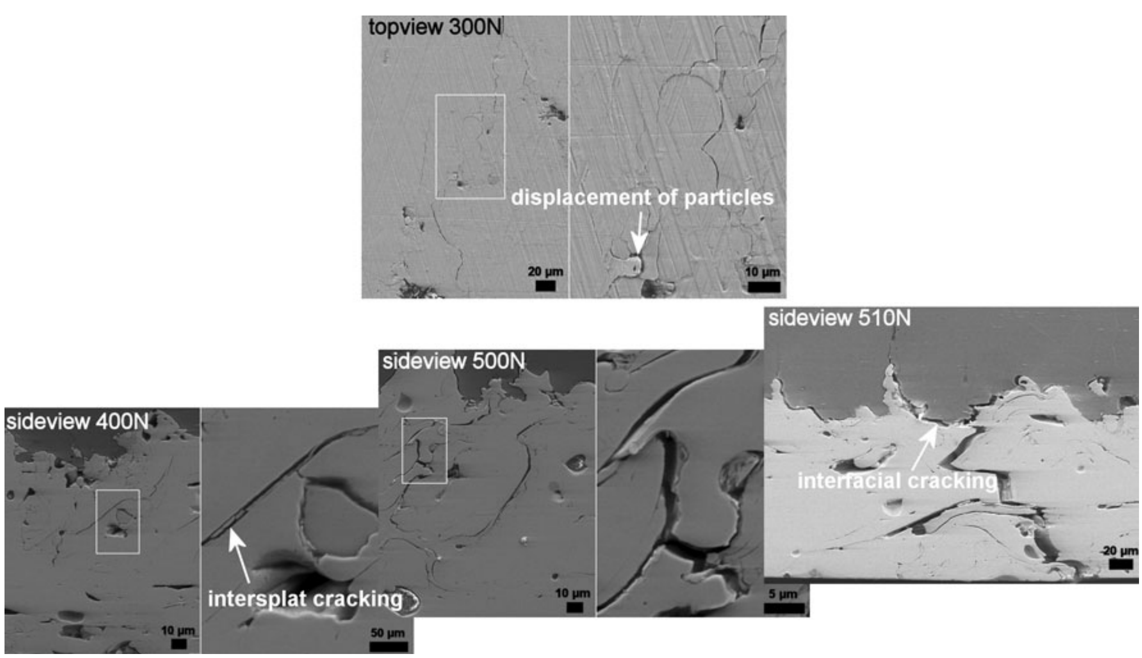

Fig. 3 Crack initiation and propagation with increased load in a TWAS FeC0.8 coating. Progressive Inter-splat cracking with increasing load (along oxide layers at splat boundaries), finally resulting in local interfacial cracks and crack propagation into the substrate

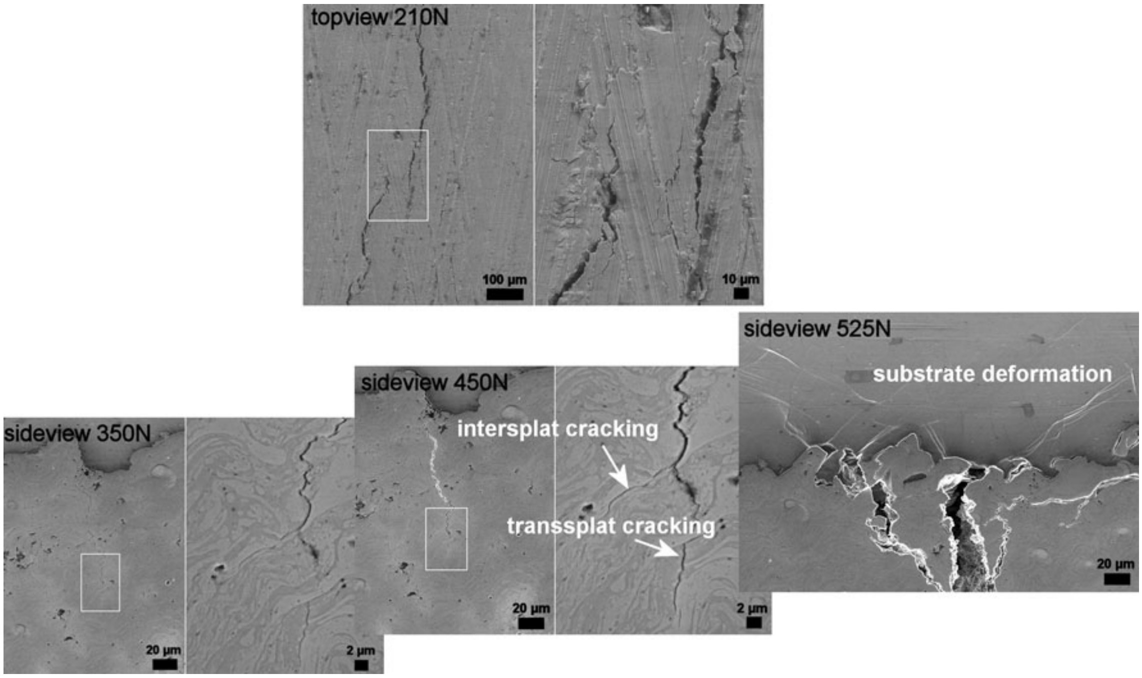

Fig. 4 Crack initiation and propagation with increased load in a HVOF FeC0.8 coating. Progressive mixed inter- and trans-splat cracking with increasing load. The substrate is highly deformed until cracks propagate into the substrate

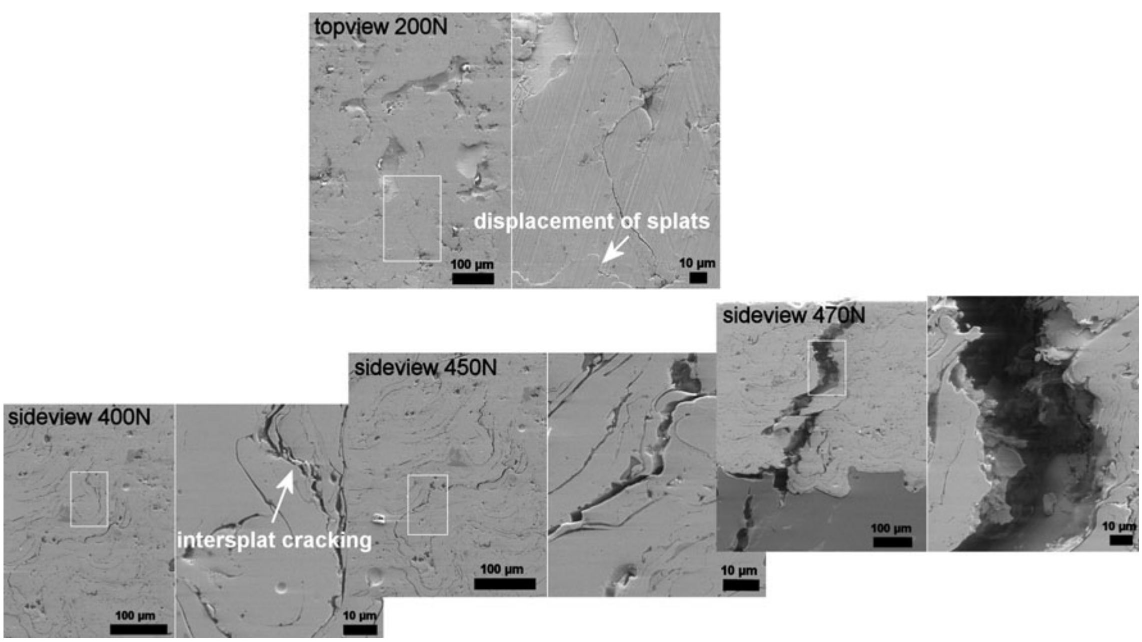

Fig. 5 Crack initiation and propagation with increased load in a PTWA FeCrCB coating. Cracks are mainly inter-splat cracks with low load, brittle microcracking leads to a mixed inter- and trans-splat cracking with further crack propagation into the substrate

of the coating (Fig. 6). The flexural stiffness is indicative for the resistance of the coated sample to bending stress. The development of the flexural stiffness over the number of cycles reveals a fluctuation of values for both tests, tensile and compression. These fluctuations assume a progressive generation of cracks. It seems that the coatings develop a large number of small cracks which do not propagate and, therefore, endanger the coating's integrity.

Large cracks could be disruptive for the coating structure either because they expose the substrate and cause

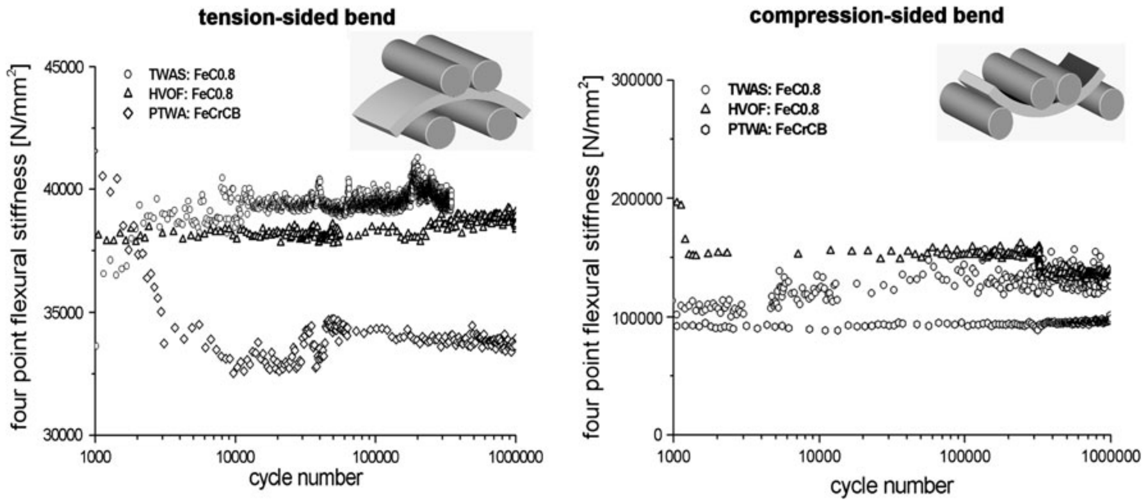

Fig. 6 Flexural stiffness for tension and compression sided bend

failure of the whole system or lead to delamination because of large interfacial cracking. The studied coatings appear to be capable of a representative deformation and tolerate a certain amount of crack initiation and propagation without destructive cracking and failure of the whole system. With a sufficient interfacial strength cracks can deflect along interfaces and therefore establish a stable system.

4. Discussion

Thermally sprayed coatings with their characteristic lamellar structure show a considerable influence of splat size, phases, and interfaces on crack initiation and propagation.

The major acting wear mechanism within cavitation is surface fatigue. Splat delamination occurs due to cracks propagating along splat interfaces. The PTWA FeCrCB coating with its amorphous or nc microstructure additionally suffers from its very low ductility.

Previous studies in tensile tests of coated materials showed that there is only a very small scope of nondestructive deformation possible in such coatings (Ref 13). The mechanical characteristics of coatings are given by locally occurring mechanisms (Ref 5). For instance local microcracking can be found repeatedly only on the scale of one individual splat consisting of a hard and brittle phase (e.g., oxides). Rabiei et al. mentioned already the critical influence of oxides in HVOF sprayed coatings for the coating performance in impact tests.

Kroupa et al. described an elastic opening and closing of the microcracks under cyclic stresses. Under tensile stresses the microcracks would grow by inelastic processes and cause a decrease in flexural stiffness (Ref 14). Therefore, compressive stresses would provoke elastic closing of microcracks and increase the flexural stiffness. Peaks or low marks in the flexural stiffness might therefore indicate significant crack initiation or propagation.

Compressive residual stresses in metal coatings are due to high velocities during deposition. Coatings with higher compressive residual stresses seem to have a higher resistance to crack initiation (Ref 15). HVOF coatings are supposed to have the highest residual stresses thus the favorably flexural stiffness with a relatively constant development during the test is comprehensible.

Tribological properties strongly depend on the grain size of the coatings. Especially the alteration of the microstructure in the contact zone reveals the ability of the material to adjust to the current load level (Ref 6, 7). Mechanical properties are determined by splat size, sufficient mechanical interlocking of splats, and adhesive bonding in the splat's interfaces.

5. Conclusions

Crack initiation and propagation in this layered composites as well as the tribological stability are investigated and brought into relation to the relevant microstructure. Splats consisting of hard phases as well as the splat's interfaces have important influence on the mechanical characteristics of these coatings. Cracks are mainly initiated in hard phases and propagate preferably along splat interfaces. Under cyclic stresses this characteristics may lead to a stable system where cracks elastically open and close without delamination of the coating or failure of the whole system. The required properties to resist against mechanical loads such as bending stresses due to the distortion of the cylinder or impact stresses due to knocking and impact of piston rings in a motor cylinder are given.

Acknowledgments

The results were derived within the NaCoLab project funded by BMBF, Berlin, Germany under Contract 03X0003K. The authors would like to thank the project partners Durum Verschleißschutz GmbH, Willich, Daimler AG, Research and Development, Ulm, IOT (Institut für Oberflächentechnik—Surface Engineering Institute), RWTH Aachen, GTV GmbH, Luckenbach, and Gehring GmbH, Ostfildern for specimens and all other partners for their steady willingness to support with information.

Peer Reviewed

References

1. R.K. Betts, Motor Vehicle Applications of Thermally Sprayed Specialty Coatings, *Proceedings of the 1st International Surface Engineering Congress and the 13th, IFHTSE, Congress of the International Federation for Heat Treatment and Surface Engineering, 13, ISEC, International Surface Engineering Congress*, 2003, Vol 1, p 716-721
2. K. Bobzin, F. Ernst, J. Zwick, T. Schläfer, D. Cook, K. Nassenstein, A. Schwenk, F. Schreiber, T. Wenz, G. Flores, and M. Hahn, Coating Bores of Light Metal Engine Blocks with a Nanocomposite Material Using the Plasma Transferred Wire Arc Thermal Spray Process, *JTST*, 2008, **17**(3), p 344-351
3. T.C. Hanson and G.S. Settles, Particle Temperature and Velocity Effects on the Porosity and Oxidation of an HVOF Corrosion-Control Coating, *JTST*, 2003, **12**(3), p 404-415
4. J. Wilden, J.P. Bergmann, S. Jahn, S. Knapp, F. van Rodijnen, and G. Fischer, Investigation About the Chrome Steel Wire Arc Spray Process and the Resulting Coating Properties, *JTST*, 2007, **16**(5-6), p 759-767
5. A. Rabiei, D.R. Mumm, J.W. Huchinson, R. Schweinfest, M. Rühle, and A.G. Evans, Microstructure, Deformation and Cracking Characteristics of Thermal Spray Ferrous Coatings, *Mater. Sci. Eng. A*, 1999, **269**(1-2), p 152-165
6. M. Hahn, R. Theissmann, B. Gleising, W. Dudzinski, and A. Fischer, Microstructural Alterations within Thermal Spray Coatings During Highly Loaded Diesel Engine Tests, *Wear*, 2009, **267**, p 916-924
7. M. Hahn, R. Theissmann, B. Gleising, W. Dudzinski, and A. Fischer, Investigation of Wear Mechanisms and Microstructural Changes of Thermally Sprayed Coatings in Cylinder Bores after Motor Tests, (Proc. Conf.) *Friction, Wear and Wear Protection*, A. Fischer and K. Bobzin, Ed., WILEY-VCH Verlag GmbH & Co. KGaA, Weinheim, Germany, 2009, p 140-151
8. C. David, K. Anthymidis, P. Agrianidis, and A. Tsipas, Determination of the Fatigue Resistance of HVOF Thermal Spray WC-CoCr Coatings by Means of Impact Testing, *JTeEv*, 2007, **35**(6), p 460-464
9. A.M. Kamara and K. Davey, A Numerical and Experimental Investigation into Residual Stress in Thermally Sprayed Coatings, *Int. J. Sol. Struct.*, 2007, **44**, p 8532-8555
10. H.-W. Hoffmeister and C. Schnell, Mechanical Roughing of Cylinder Bores in Light Metal Crankcases, Production Engineering: Research and Development, *Ann. German Acad. Soc. Product. Eng.*, 2007, **2**(4), p 365-370
11. U. Köster and U. Herold, Comments on Chemical Ordering in Some Amorphous Alloys, *Mater. Sci. Eng.*, 1980, **45**(3), p 285-287
12. M. Hahn and A. Fischer, Characterization of Thermally Sprayed Micro- and Nanocrystalline Cylinder Wall Coatings by Means of a Cavitation Test, *J. Eng. Tribol. J*, 2009, **223**(1), p 27-37
13. Y. Shinara, R. Wang, T. Tokuda, M. Kido, Y. Harada, and S. Wada, Surface Strain Measurement of Thermally Sprayed Ceramic Coatings Under Static and Cyclic Loadings and its Application to Detection of Delamination, *Mater. Trans.*, 2007, **48**(4), p 769-774
14. F. Kroupa, Nonlinear Behaviour in Compression and Tension of Thermally Sprayed Ceramic Coatings, *JTST*, 2007, **16**(1), p 84-95
15. S. Bouaricha, J.-G. Gegoux, and P. Marcoux, Bending Behaviour of HVOF Produced WC-17Co Coating: Investigated by Acoustic Emission, *JTST*, 2004, **13**(3), p 405-413